CARBON 76 (2014) 148–154

Available at www.sciencedirect.com

ScienceDirect

journal homepage: www.elsevier.com/locate/carbon

# Chemically engineered graphene oxide as high performance cathode materials for Li-ion batteries

Wei Ai [a], Zhuzhu Du [b], Zhanxi Fan [c], Jian Jiang [a], Yanlong Wang [a], Hua Zhang [c], Linghai Xie [b], Wei Huang [b,e,*], Ting Yu [a,d,f,*]

[a] Division of Physics and Applied Physics, School of Physical and Mathematical Sciences, Nanyang Technological University, 637371, Singapore

[b] Key Laboratory for Organic Electronics & Information Displays (KLOEID) and Institute of Advanced Materials (IAM), Nanjing University of Posts and Telecommunications, 9 Wenyuan Road, Nanjing 210046, PR China

[c] School of Materials Science and Engineering, Nanyang Technological University, 639798, Singapore

[d] Graphene Research Centre, National University of Singapore, 117546, Singapore

[e] Jiangsu-Singapore Joint Research Center for Organic/Bio-Electronics & Information Displays and Institute of Advanced Materials, Nanjing Tech University, Nanjing 211816, PR China

[f] Department of Physics, Faculty of Science, National University of Singapore, 117542, Singapore

ARTICLE INFO

*Article history:*
Received 14 March 2014
Accepted 16 April 2014
Available online 28 April 2014

ABSTRACT

The development of environment-friendly electrode materials is highly desired for the clean and sustainable Li-ion batteries (LIBs) system. Organic cathode materials that involve conducting polymers, organic carbonyl/sulfur compounds are expected to be promising candidates for future LIBs with a concept of "green and sustainable". However, their battery performances are relatively worse than that of inorganic counterparts due to their low electronic conductivity and unwanted dissolution reactions occurring in electrolytes. Aimed to alter their performances, we herein focuses on the preparation of upgraded organic materials by chemical engineering of graphene oxide (GO) and the systematic study of their electrochemical performance as positive electrodes for LIBs. The obtained decarboxylated GO and carbonylated/hydroxylated GO electrodes show significantly enhanced electrochemical performance compared with that of the GO electrode. Our results demonstrate that the manipulation of oxygen functional groups on GO is an effective strategy to greatly improve the Li storage property of GO-based materials for advanced LIBs cathodes.



## 1. Introduction

Tackling energy conversion/storage is unquestionably one of the greatest challenges in the twenty-first century. In response to the needs of modern society and sustainable concepts, the rapid development of energy conversion and storage technologies with high-efficiency, low-cost and environment-friendly is required essentially [1,2]. Among various

* *Corresponding authors*. Address: Key Laboratory for Organic Electronics & Information Displays (KLOEID) and Institute of Advanced Materials (IAM), Nanjing University of Posts and Telecommunications, 9 Wenyuan Road, Nanjing 210046, PR China (W. Huang). Address: Division of Physics and Applied Physics, School of Physical and Mathematical Sciences, Nanyang Technological University, 637371, Singapore. Fax: +65 63167899 (T. Yu).

E-mail address: yuting@ntu.edu.sg (T. Yu).

http://dx.doi.org/10.1016/j.carbon.2014.04.061
0008-6223/

energy-storage techniques, Li-ion batteries (LIBs) are the most promising candidate, especially as the power source for plug-in hybrid and electrical vehicles due to their large energy-storage capability [3]. Current LIBs technology relies on the use of active inorganic materials (e.g., $LiCoO_2$, $LiNiO_2$ or $LiFePO_4$) as cathodes due to the high redox potential of these lithium transition metal oxides or phosphates [4]. However, the energy storage using this strategy has been demonstrated to be mainly restricted by the cathode materials which usually have much high molecular weight, thus limiting the practical capacity in a range of 150–200 mAh $g^{-1}$ [5]. Also, the preparation of the cathodes is not environmentally benign since it involves high temperature reactions and yields high amounts of $CO_2$ [6]. Moreover, the expanding application of LIBs significantly increases the running out of the limited mineral resources of Co and Ni that are far from renewable in the future. Meanwhile, the scarcity of these elements makes the energy intensive, which is going to increase with their rarefaction in future [7]. Thus, there is intense interest in finding new advanced cathode materials that combined with high capacity and high stability while being with low-cost and environment-friendly [5].

In comparison to conventional inorganic materials, the organic cathode materials typically like conducting polymers [8], organic carbonyl compounds [9] and organosulfur compounds [2] have also been rapidly developed recently due to their higher energy density/power density than inorganic cathodes. Organic cathodes have some special advantages over the inorganic ones: (i) The structural diversity of organic endows great opportunities for the adjustment of physicochemical properties/structures of cathode materials. In contrast, very few kinds of inorganic materials are suitable for the application of cathode electrodes; in addition, the development of future inorganic cathodes with breakthroughs on energy/power densities becomes more and more challenging [5,10]. (ii) High-temperature annealing treatments on inorganic cathodes for their phase-purity/crystallinity are not required for the case of organics because they can be synthesized from abundant/renewable biomass resources. With that, low $CO_2$ production and far less energy consumption would enable the concept of "green and sustainable" LIBs possible [7,11]. Unfortunately, the electrochemical performances of organic cathodes are worse than inorganic ones because of their poor electronic conductivity and chemical stability in the electrolyte [10,12]. Graphene oxide (GO) is considered as a large, disordered but two-dimensional polymer that is functionalized with various oxygen-containing groups, like carbonyl/carboxyl groups at the edge and hydroxyl/epoxy groups on the basal plane [2,13]. Recent studies have further demonstrated that Li storage properties of GO-based cathodes are much sensitive to the nature of oxygen-functional groups [14,15]. Hence, it is appealing to construct GO-based cathodes by combining the stable and highly conducting graphene framework for electron transport and anchored electroactive functional groups for Li storage.

We herein report novel strategies for the fabrication of carbonylated/hydroxylated graphene oxide (C/HGO) and decarboxylated graphene oxide (DCGO) via the selective removal of the oxygen functional groups on GO. The resultant C/HGO and DCGO are proved to be superior cathode materials, showing a high potential (vs. $Li/Li^+$) for LIBs and significantly enhanced Li storage properties when compared with the pristine GO. There is a special highlight that C/HGO exhibits much better electrochemical performances than conventional $LiCoO_2$ and $LiFePO_4$ cathodes, with upper capacity, good rate capability and excellent cycling behavior, which is mainly due to the derived framework structures for electron transport together with abundant carbonyl/hydroxyl functional groups beneficial for Li storage. We believe that the functionalized GO materials made by our facile chemically engineered method may open up an opportunity to develop high-performance GO-based cathodes for future LIBs with high energy density.

## 2. Experimental

### 2.1. Materials

Graphite powder (325 mesh) was purchased from Baichuan Graphite Co., Ltd. (Qingdao, China). Sulfuric acid ($H_2SO_4$), potassium permanganate ($KMnO_4$), hydrogen peroxide ($H_2O_2$), tetrahydrofuran (THF), N,N-Dimethylformamide (DMF), Potassium carbonate ($K_2CO_3$), Silver nitrate ($AgNO_3$) and n-Butyllithium (BuLi) were purchased from Sinopharm Chemical Reagent Co., Ltd. (Shanghai, China).

### 2.2. Synthesis of GO

GO was synthesized from natural graphite by a modified Hummers' method according to our previous reports [16].

### 2.3. Synthesis of DCGO

DCGO was prepared via chemoselective decarboxylation of GO [17]. GO (500 mg) was dispersed in 300 mL DMF by ultrasonication, then $K_2CO_3$ (460 mg) and $AgNO_3$ (330 mg) were added under stirring. The mixture was stirred at 80 °C for 16 h. Afterwards, the product was collected by centrifugation, and washed with 30% $HNO_3$ for 4 times, then washed with deionized water for several times, and finally dried under vacuum condition.

### 2.4. Synthesis of C/HGO

GO (1.0 g) was added into 200 mL of anhydrous THF under stirring, and then 40 mL BuLi was dropwised under $N_2$ condition. The mixture was stirred at room temperature for 24 h. Subsequently, the suspension was centrifugated and washed with deionized water for several times, and finally dried under vacuum condition.

### 2.5. Characterization

Fourier transformed infrared spectra (FT-IR) were spectra were recorded on a NEXUS 670 spectrometer by using pressed KBr pellets. X-ray photoelectron spectroscopy (XPS) analysis was performed on an ESCALAB MK II X-ray photoelectron spectrometer using Al Kα (1486.6 eV) X-ray source. Field-emission scanning electron microscopy (FESEM) analysis was

performed on a JEOL JSM-6700F electron microscope with an accelerating voltage of 10 kV. Transmission electron microscopy (TEM) images were taken on a JEOL JEM-2010 high resolution transmission electron microscope operating at 200 kV. X-ray diffraction (XRD) analysis was performed using a D8 Advanced diffractometer with Cu Kα line ($\lambda = 1.54056$ Å). Raman spectra were collected using a WITEC CRM200 Raman system with 532 nm excitation laser. Thermogravimetric analysis (TGA) was recorded by a Shimadzu DTG-60H under a heating rate of 10 °C $min^{-1}$ and a nitrogen flow rate of 50 $cm^3$ $min^{-1}$.

### 2.6. Electrochemical measurements

The electrochemical characterizations were performed using 2032 coin-type cells assembled inside an argon-filled glove box with both moisture and oxygen contents below 0.1 ppm. The working electrodes were made by coating the slurry of 80 wt% active material, 10 wt% of acetylene black and 10 wt% of polyvinylidene fluoride onto an aluminium foil current collector. Then, they were dried in a vacuum oven at 100 °C for 12 h to remove the solvent. Lithium metal foil was used as the counter electrode. The electrolyte is composed of 1 M $LiPF_6$ in a 50:50 (w/w) mixture of ethylene carbonate and dimethyl carbonate. The galvanostatic charge/discharge tests were performed using a NEWARE battery testing system in the voltage range of 1.5–4.5 V (vs. $Li/Li^+$). Cyclic voltammogram (CV) measurements were performed on CHI 760D electrochemical workstation using a voltage range of 1.5–4.5 V (vs. $Li/Li^+$) at a scan rate of 0.2 mV $s^{-1}$. Electrochemical impedance spectroscopy (EIS) was conducted on CHI 760D electrochemical workstation in the frequency range of $1 \times 10^5$–0.1 Hz.

## 3. Results and discussion

A general description of the methods used to synthesize DCGO and C/HGO is illustrated in Fig. 1. The synthesis of DCGO involves the chemoselective decarboxylation of GO, while C/HGO was prepared via the n-Butyllithium-promoted carbonylation/hydroxylation of GO, which are both described in the Section 2 for details. A comprehensive structural analysis was carried out to ensure that the chemoselective decarboxylation and carbonylation/hydroxylation of GO were successfully completed.

XPS was employed for chemical analysis of surface functional groups on graphene sheets. In Fig. 2a, the C1s core-level spectrum of GO was fitted into four components that correspond to C–C bonds ($sp^2$ carbon, 284.5 eV, 42.5%), C–O bonds (hydroxyl and epoxy, 286.6 eV, 47.9%), C=O bonds (carbonyl, 288.1 eV, 7.0%) and O–C=O bonds (carboxyl, 288.9 eV, 2.6%) [13]. After the chemoselective decarboxylation, the peak intensity of C–O bonds in DCGO are comparable to the value of pristine GO, together with the intensity of O–C=O bonds reduced by ~100% (Fig. 2b). The slightly increased intensity of C–C bonds (50.6%) could be attributed to the removal of carboxyl groups, which results in a partial reduction of GO. While C/HGO exhibits an obviously reduced peak intensity of C–O bonds (21.9%) and O–C=O bonds (0%), and the intensity of C=O bonds is increased to 9.4% after n-Butyllithium-promoted carbonylation/hydroxylation (Fig. 2c). Meanwhile, a significantly increased peak intensity of C–C bonds (68.7%) is also observed in C/HGO due to the partial reduction of GO after the carbonylation/hydroxylation process. It is worthy of note that the C1s/O1s atomic ratios of GO, DCGO and C/HGO are 2.0, 2.6 and 3.2, respectively, suggesting that the n-Butyllithium-promoted carbonylation/hydroxylation is more effective in removal of the oxygen-containing groups on GO than the chemoselective decarboxylation.

To further gain more insight into the chemical composition of the as-obtained DCGO and C/HGO, FT-IR, TGA, XRD and Raman spectroscopy were used to analyze their structural properties. Fig. 2d shows the typical FT-IR spectrum of GO, the adsorption bands at ~1730, ~1620 and ~1229 $cm^{-1}$, corresponding to the C=O, C=C and C–O stretching vibrations, respectively [18]. Surprisingly, DCGO exhibits similar FT-IR spectrum to that of GO, except for the decreased intensity of C=O bonds due to the chemoselective decarboxylation. In comparison to GO and DCGO, some of the oxygen-containing functional groups changes as reflected by the corresponding spectral features such as frequency and/or intensity in the spectrum of C/HGO after the carbonylation/hydroxylation process. The weak adsorption band at ~1716 $cm^{-1}$ suggests the presence of new carbonyl species, which can be assigned to the stretching vibration of conjugated ketones that derived from the carboxyl groups [19]. In addition, the upshift of the C–O adsorption band with relative low intensity is also observed. Moreover, the new adsorption bands at ~1596, ~1493 and ~1436 $cm^{-1}$ are ascribed to the skeletal vibrational mode of the benzene ring from graphene, while the peak at ~860 $cm^{-1}$ is due to the C–H bending vibration [20]. These results are consistent with the XPS results, indicating the successful fabrication of DCGO and C/HGO after the chemoselective decarboxylation and the n-Butyllithium-promoted carbonylation/hydroxylation of GO, respectively.

Fig. 2e shows the TGA curves of GO, DCGO and C/HGO. It can be observed that the thermal stability of DCGO and C/HGO was enhanced after the chemical manipulation of GO through the chemoselective decarboxylation and the n-Butyllithium-promoted carbonylation/hydroxylation. All these materials have initial mass loss even below 100 °C,

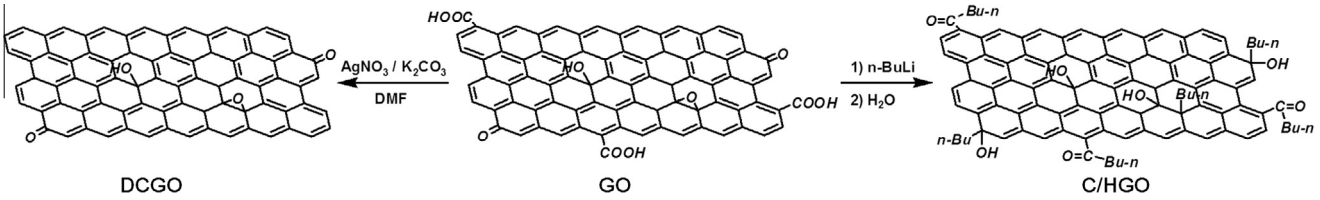


**Fig. 1 – Schematic illustration of the synthesis of DCGO and C/HGO.**

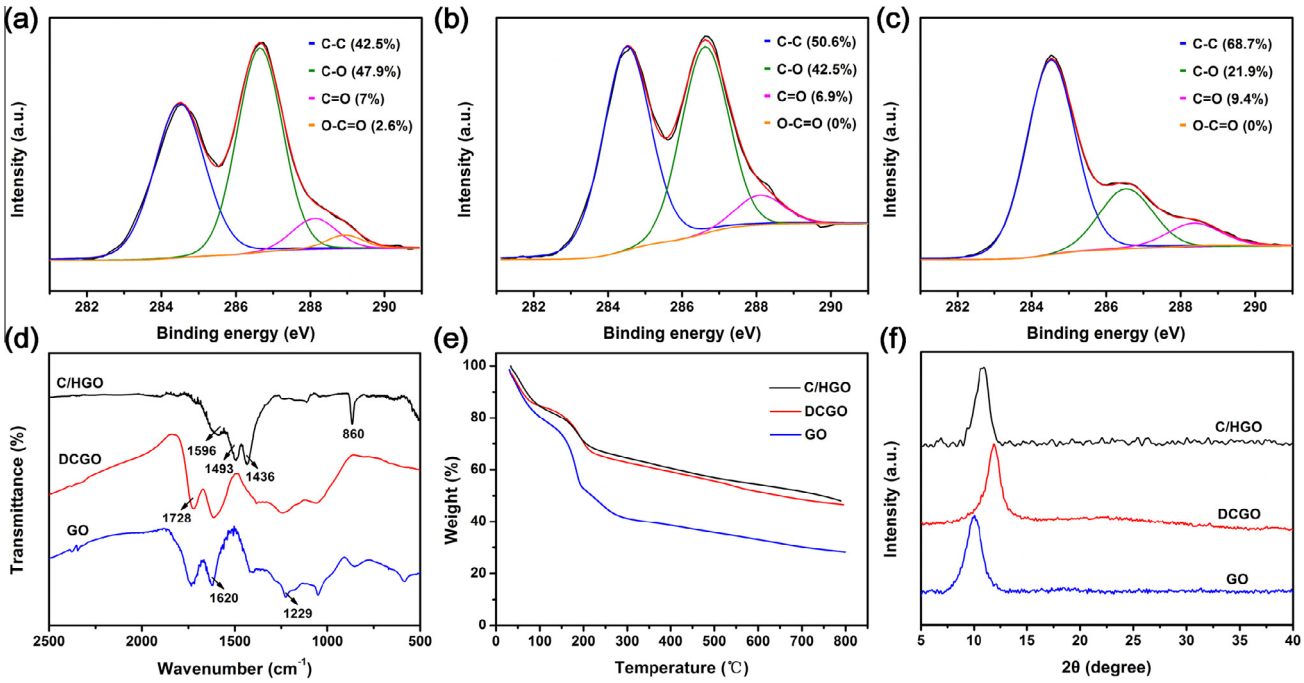


**Fig. 2 – The C1s XPS spectra of (a) GO, (b) DCGO and (c) C/HGO. (d) FT-IR spectra of GO, DCGO and C/HGO. (e) TGA curves of GO, DCGO and C/HGO. (f) XRD patterns of GO, DCGO and C/HGO. (A color version of this figure can be viewed online.)**

assigned to the evaporation of water molecular trapped in the π-stacked graphene sheets [21]. And the rate of mass loss increased in the heating period of 100–200 °C due to the decomposition of the labile oxygen-containing functional groups, yielding CO, $CO_2$ and steam [13]. However, compared to GO, the mass loss with temperature in the range of 100–200 °C for DCGO and C/HGO is significantly lower, and smaller mass loss are observed, indicating the partial removal of the oxygen functional groups after the chemoselective decarboxylation and carbonylation/hydroxylation of GO, as confirmed by XPS analysis. Moreover, XRD patterns were used to further study the structural properties of these materials as shown in Fig. 2f. The interlayer distance of DCGO and C/HGO is calculated to be 7.49 and 8.18 Å, respectively, which is much lower than that of GO precursor (8.85 Å). The decreased interlayer distance could be attributed to the partial removal of the oxygen functional groups on GO that will induce a weakened electrostatic repulsion between the graphene sheets. These results have also been confirmed by TGA and XPS analysis. Raman spectra of all these materials show two typical peaks, one is the defects or disorders induced D band at ~1350 $cm^{-1}$, while another one is the tangential G band mode at ~1600 $cm^{-1}$ (Fig. S1). Meanwhile, the frequency of the D and G band in DCGO and C/HGO are very similar to that observed in GO. It is seen that the $I_D/I_G$ ratio of DCGO and C/HGO is slightly larger in comparison with that of GO, which could be assigned to the decrease in size of $sp^2$ domains and a partially ordered crystal structure after the chemical reaction engineering processes [22].

Fig. 3a shows the FESEM image of GO with a typically crumpled morphology, which is in agreement with previous studies [23]. The SEM images in Fig. 3b and c reveal that the DCGO and C/HGO exhibit a thin and graphite-like structure due to the weakened electrostatic repulsion between the graphene sheets after partial removal of the oxygen functional groups. Meanwhile, pore structures with several micrometers are also clearly observed in the SEM images of DCGO and C/HGO, which are formed by the interconnected graphite-like structure. Such feature is favorable for the better access of the electrolyte, thus facilitating the rapid diffusion of Li-ions from electrolyte to the electrode materials. Moreover, the electrolyte can also penetrate into the electrode materials due to the large interlayer distance of these materials (comparing to graphite) that caused by the intercalation of oxygen-containing functional groups on the graphene sheets, as demonstrated by XRD patterns (Fig. 2f). These characteristics can ensure the fast Faradaic reaction of the electroactive functional groups with Li-ions, especially at high charge/discharge rates. In addition, some small dots are observed in the SEM image of DCGO, which may correspond to the silver-based nanoparticles that induced during the chemoselective decarboxylation process. However, it has no influence on the final electrochemical performance of the DCGO because Li insertion into silver is below 0.1 V (vs. $Li/Li^+$) [24]. TEM was used to further investigate the morphology of C/HGO. As shown in Fig. 3d, C/HGO exhibits a stacked layer structure (inset of Fig. 3d) as appearing in the SEM image. High-resolution TEM (HRTEM) clearly indicates the recovery of graphitic carbon structures in C/HGO, which can act as the channels for electron transport, while the remaining C=O and –OH surface functional groups can serve as the Faradaic reactions centers for efficient Li storage.

The electrochemical performance of these GO-based materials was tested in a CR-2032 type coin cell by using the standard half-cell configuration. Figs. 4a and S2 show the CV curves of the three samples. It can be seen that the DCGO

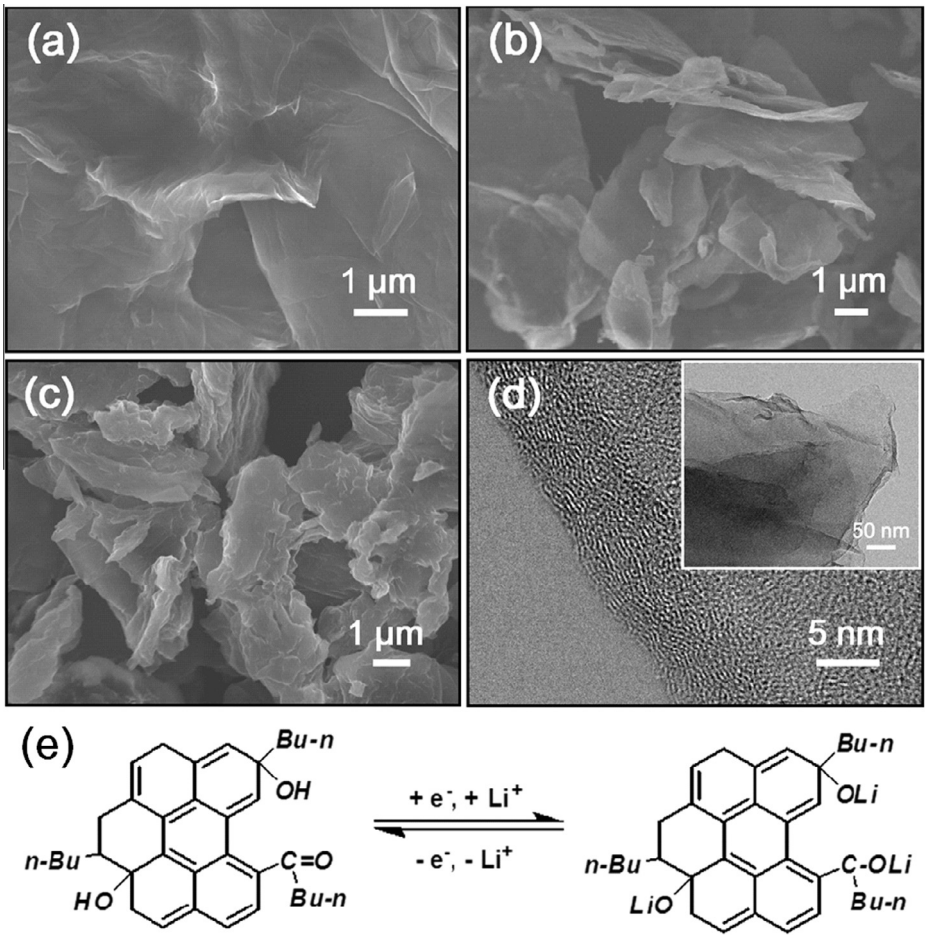


**Fig. 3 – FESEM images of (a) GO, (b) DCGO and (c) C/HGO. (d) HRTEM image of C/HGO. Inset shows the TEM image of C/HGO. (e) Schematic illustration of the Faradaic reactions on the C/HGO electrodes.**

and C/HGO electrodes show a reversible lithiation/delithiation process and better resolved CV peaks, but the reversibility of GO is quite poor due to the irreversible cleavage of the oxygen functional groups [25]. In the initial cycle, a couple of redox peaks is observed at about 1.7/4.2 for DCGO and 1.8/4.2 for C/HGO, resulting from the lithiation/delithiation process between $Li^+$ and the carbonyl, hydroxyl and epoxy groups on the electrode materials [26]. However, the cathodic peak of these two materials shifts to a higher potential at ~2.2 V in the following cycles, indicating an improved reversibility of the electrochemical reaction with cycling due to the reduced hysteresis between the anodic and cathodic peaks [27]. Galvanostatic charge/discharge testing of these GO-based electrodes at various current densities with a voltage range from 1.5 to 4.5 V are shown in Figs. 4b and S3. Notably, the discharge capacity of C/HGO is always higher than that of GO and DCGO electrodes under the same current density. For example, the average discharge capacity of C/HGO is 175 mAh $g^{-1}$ at a current density of 100 mA $g^{-1}$ (Fig. 4c), while GO and DCGO electrodes show an average capacity of 55 and 107 mAh $g^{-1}$, respectively. Moreover, the C/HGO always exhibits a much larger capacity throughout the whole cycling testing. It is interesting to note that the capacity of GO and DCGO in the first cycle is comparable to C/HGO, then gradually decreased in the following few cycles. This phenomenon might be derived from the irreversible cleavage of the oxygen functional groups that has also been demonstrated in the CV test [25,26]. The capacity increasing of the DCGO after certain cycles could be attributed to the activating process of the electrode, which has also been observed in other carbon-based materials [28,29]. In contrast, the C/HGO shows much improved cycling stability over 600 cycles, indicating the manipulation of the oxygen functional groups on GO is indeed an effective strategy to decrease the irreversible lithiation process of GO-based electrodes while enabling high potential (vs. $Li/Li^+$) and significantly enhanced Li storage properties. Moreover, the remarkably enhanced conductivity of C/HGO, demonstrated by XPS analysis and the EIS, can also be responsible for its higher capacity. As shown in Fig. S4, comparing with GO and DCGO electrodes, the C/HGO electrode shows lower bulk resistance $R_b$ (electrolyte resistance, contact resistance…) and lower charge transfer resistance $R_{CT}$ (GO (126.4 Ω) < DCGO (111.3 Ω) < C/HGO (70.9 Ω)), as well as lower Warburg impedance $Z_w$ that related to the diffusion of $Li^+$ into the bulk electrode.

To further exploit advantages of the chemical engineering of GO, a potential pathway for the tailoring of Li storage properties in GO, the rate performance of the as-obtained GO-based materials is also investigated (Figs. 4d and S5). Obviously, with respect to the reference GO cathode, the

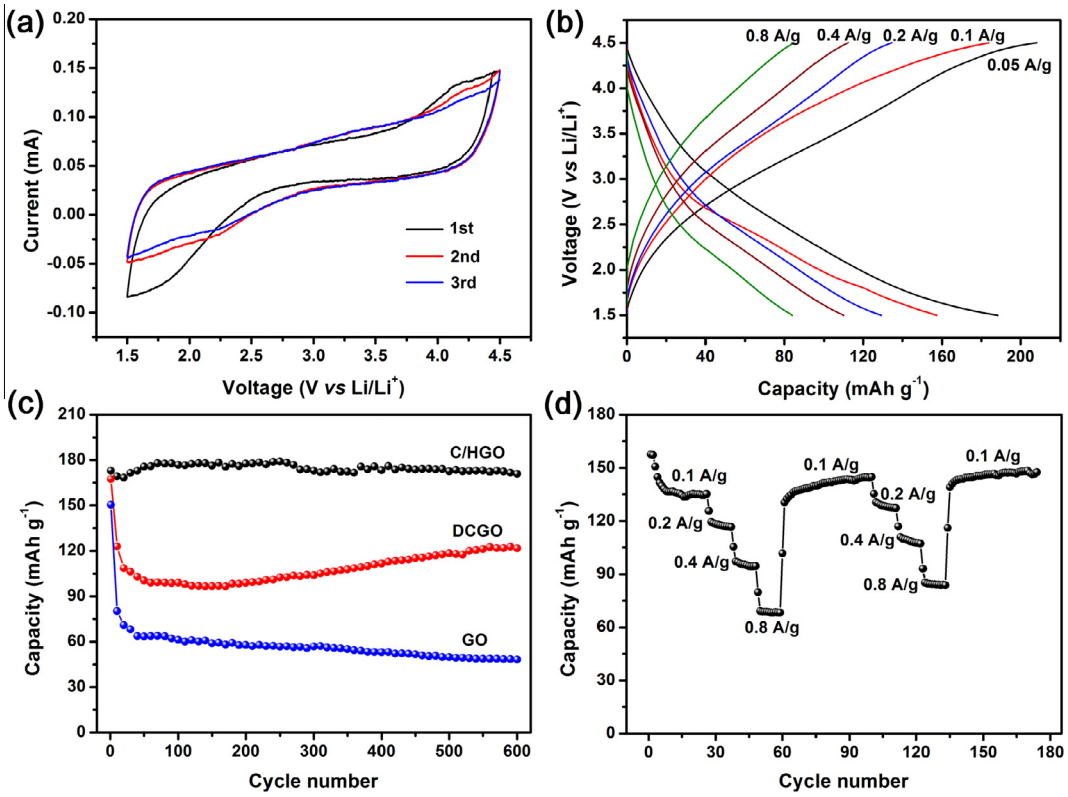


**Fig. 4 – (a) CV curves of C/HGO electrode at a scan rate of 0.2 mV $s^{-1}$. (b) Charge–discharge curves of C/HGO electrode at various current densities. (c) Cycling performance of GO, DCGO and C/HGO electrodes at a current density of 100 mA $g^{-1}$. (d) Rate capability of C/HGO electrode at different rates. (A color version of this figure can be viewed online.)**

specific capacity of the DCGO and C/HGO is substantially increased at all investigated charge–discharge rates from 100 to 800 mA $g^{-1}$. Especially, the C/HGO cathode exhibits much superior rate performance with good capacity retention. The discharge capacity of C/HGO at a rate of 800 mA $g^{-1}$ is as high as 84 mAh $g^{-1}$, which is close to two times of that of GO electrode (45 mAh $g^{-1}$) and over three times of that of DCGO (24 mAh $g^{-1}$). Moreover, even after extended rate cycles at the high rate measurements, the high capacity of C/HGO cathode at 100 mA $g^{-1}$ can also be recovered to almost the initial value, suggesting its good reversibility. At the high current rates (400 and 800 mA $g^{-1}$), DCGO exhibits a lower capacity to that of GO, which can be ascribed to its long activating process as observed in its cycling test in Fig. 4c.

The increased capacity, long-term cycling stability and high rate capability of the C/HGO electrode are attributed to its novel structure. As illustrated in Fig. 3d and e, the graphene framework of the C/HGO can serve as channels for electron transport, whereas the remaining hydroxyl and carbonyl groups in C/HGO may act as the reservoirs for Li storage [27]. Therefore, the electrode can easily contact with the electrolyte, ensuring fast Faradaic reaction of the electroactive functional groups with Li-ions and rapid charge transfer reaction. Also, this feature will shorten the diffusion length of Li-ions and fasten Li-ions diffusion from electrolyte to electrode. On the other hand, the much decreased oxygen content in C/HGO endows its high electrical conductivity, which will provide a fast and efficient pathway for electron transfer between the active materials and the current collector. Comparing with other reported organic carbonyl compounds cathode materials, the excellent electrochemical performance of the C/HGO is attributed to (i) its insolubility in the electrolyte, (ii) good conductivity for electron transport, (iii) abundant hydroxyl and carbonyl groups for Li storage, implying its great potential as a promising cathode material for high-performance energy storage applications.

## 4. Summary

We have demonstrated that high-performance GO-based cathodes can be successfully fabricated via chemical engineering of GO. The effectiveness of this strategy is to construct highly conducting graphene framework with electroactive functional groups for reversible and fast Li storage through chemoselective removal of the oxygen functional groups on GO. The novel structure of the obtained GO-based cathodes grantees these materials being superior to the conventional Li intercalation cathodes, such as lithium transition metal oxides or phosphates [30,31]. Especially, C/HGO cathode exhibits excellent electrochemical performance in terms of high capacity, good rate capability and cycling stability. We believe that this chemical engineering strategy could be broadly applicable for the fabrication of other carbon-based cathodes for next-generation high-performance LIBs.

## Acknowledgments

This work is supported by the Singapore National Research Foundation under NRF RF Award No. NRFRF2010-07, A*Star SERC PSF Grant 1321202101 and MOE Tier 2 MOE2012-T2-2-049. H.Z. thanks the support from Singapore MOE under AcRF Tier 2 (ARC 26/13, No. MOE2013-T2-1-034) and AcRF Tier 1 (RG 61/12), and the Start-Up Grant (M4080865.070.706022) in NTU. This research is also funded by the Singapore National Research Foundation and the publication is supported under the Campus for Research Excellence and Technological Enterprise (CREATE) programme (Nanomaterials for Energy and Water Management).

## Appendix A. Supplementary data

Supplementary data associated with this article can be found, in the online version, at http://dx.doi.org/10.1016/j.carbon.2014.04.061.

## REFERENCES

[1] Sathiya M, Rousse G, Ramesha K, Laisa CP, Vezin H, Sougrati MT, et al. Reversible anionic redox chemistry in high-capacity layered-oxide electrodes. Nat Mater 2013;12(9):827–35.
[2] Ai W, Xie L, Du Z, Zeng Z, Liu J, Zhang H, et al. A novel graphene-polysulfide anode material for high-performance lithium-ion batteries. Sci Rep 2013;3:2341.
[3] Reddy ALM, Gowda SR, Shaijumon MM, Ajayan PM. Hybrid nanostructures for energy storage applications. Adv Mater 2012;24(37):5045–64.
[4] Whittingham MS, Song Y, Lutta S, Zavalij PY, Chernova NA. Some transition metal (oxy)phosphates and vanadium oxides for lithium batteries. J Mater Chem 2005;15(33):3362–79.
[5] Xu B, Qian D, Wang Z, Meng YS. Recent progress in cathode materials research for advanced lithium ion batteries. Mater Sci Eng 2012;73(5–6):51–65.
[6] Armand M, Tarascon JM. Building better batteries. Nature 2008;451(7179):652–7.
[7] Chen H, Armand M, Demailly G, Dolhem F, Poizot P, Tarascon JM. From biomass to a renewable $Li_xC_6O_6$ organic electrode for sustainable Li-ion batteries. ChemSusChem 2008;1(4):348–55.
[8] Janoschka T, Teichler A, Häupler B, Jahnert T, Hager MD, Schubert US. Reactive inkjet printing of cathodes for organic radical batteries. Adv Energy Mater 2013;3(8):1025–8.
[9] Huang W, Zhu Z, Wang L, Wang S, Li H, Tao Z, et al. Quasi-solid-state rechargeable lithium-ion batteries with a Calix[4]quinone cathode and gel polymer electrolyte. Angew Chem Int Ed 2013;52(35):9162–6.
[10] Song Z, Zhou H. Towards sustainable and versatile energy storage devices: an overview of organic electrode materials. Energy Environ Sci 2013;6(8):2280–301.
[11] Chen H, Armand M, Courty M, Jiang M, Grey CP, Dolhem F, et al. Lithium salt of tetrahydroxybenzoquinone: toward the development of a sustainable Li-ion battery. J Am Chem Soc 2009;131(25):8984–8.
[12] Liang Y, Tao Z, Chen J. Organic electrode materials for rechargeable lithium batteries. Adv Energy Mater 2012;2(7):742–69.
[13] Ai W, Liu JQ, Du ZZ, Liu XX, Shang JZ, Yi MD, et al. One-pot, aqueous-phase synthesis of graphene oxide functionalized with heterocyclic groups to give increased solubility in organic solvents. RSC Adv 2013;3(1):45–9.
[14] Wang DW, Sun C, Zhou G, Li F, Wen L, Donose BC, et al. The examination of graphene oxide for rechargeable lithium storage as a novel cathode material. J Mater Chem A 2013;1(11):3607–12.
[15] Kim H, Lim HD, Kim SW, Hong J, Seo DH, Kim DC, et al. Scalable functionalized graphene nano-platelets as tunable cathodes for high-performance lithium rechargeable batteries. Sci Rep 2013;3:1506.
[16] Ai W, Zhou W, Du Z, Du Y, Zhang H, Jia X, et al. Benzoxazole and benzimidazole heterocycle-grafted graphene for high-performance supercapacitor electrodes. J Mater Chem 2012;22(44):23439–46.
[17] Du ZZ, Li W, Ai W, Tai Q, Xie LH, Cao Y, et al. Chemoselective reduction of graphene oxide and its application in nonvolatile organic transistor memory devices. RSC Adv 2013;3(48):25788–91.
[18] Marcano DC, Kosynkin DV, Berlin JM, Sinitskii A, Sun Z, Slesarev A, et al. Improved synthesis of graphene oxide. ACS Nano 2010;4(8):4806–14.
[19] Guo Z, Reddy MV, Goh BM, San AKP, Bao Q, Loh KP. Electrochemical performance of graphene and copper oxide composites synthesized from a metal-organic framework (Cu-MOF). RSC Adv 2013;3(41):19051–6.
[20] Bao Q, Zhang H, Yang JX, Wang S, Tang DY, Jose R, et al. Graphene-polymer nanofiber membrane for ultrafast photonics. Adv Funct Mater 2010;20(5):782–91.
[21] Ai W, Du ZZ, Liu JQ, Zhao F, Yi MD, Xie LH, et al. Formation of graphene oxide gel via the [small pi]-stacked supramolecular self-assembly. RSC Adv 2012;2(32):12204–9.
[22] Zhu C, Guo S, Fang Y, Dong S. Reducing sugar: new functional molecules for the green synthesis of graphene nanosheets. ACS Nano 2010;4(4):2429–37.
[23] Liang K, Hongkun H, Chao G. Click chemistry approach to functionalize two-dimensional macromolecules of graphene oxide nanosheets. Nano-Micro Lett 2010;2(2):177–83.
[24] Taillades G, Sarradin J. Silver: high performance anode for thin film lithium ion batteries. J Power Sources 2004;125(2):199–205.
[25] Mermoux M, Touzain P. Lithium graphitic oxide cells. Part V. An all-solid-state battery using graphite oxide as active cathodic material. J Power Sources 1989;26(3–4):529–34.
[26] Byon HR, Gallant BM, Lee SW, Yang SH. Role of oxygen functional groups in carbon nanotube/graphene freestanding electrodes for high performance lithium batteries. Adv Funct Mater 2013;23(8):1037–45.
[27] Reddy ALM, Nagarajan S, Chumyim P, Gowda SR, Pradhan P, Jadhav SR, et al. Lithium storage mechanisms in purpurin based organic lithium ion battery electrodes. Sci Rep 2012;2:960.
[28] Qie L, Chen WM, Wang ZH, Shao QG, Li X, Yuan LX, et al. Nitrogen-doped porous carbon nanofiber webs as anodes for lithium ion batteries with a superhigh capacity and rate capability. Adv Mater 2012;24(15):2047–50.
[29] Du ZZ, Ai W, Xie LH, Huang W. Organic radical functionalized graphene as a superior anode material for lithium-ion batteries. J Mater Chem A 2014. http://dx.doi.org/10.1039/C4TA00345D.
[30] Jung YS, Lu P, Cavanagh AS, Ban C, Kim GH, Lee SH, et al. Unexpected improved performance of ALD coated $LiCoO_2$/graphite Li-ion batteries. Adv Energy Mater 2013;3(2):213–9.
[31] Guo CX, Shen YQ, Dong ZL, Chen XD, Lou XW, Li CM. DNA-directed growth of $FePO_4$ nanostructures on carbon nanotubes to achieve nearly 100% theoretical capacity for lithium-ion batteries. Energy Environ Sci 2012;5(5):6919–22.